

1

2 **Network controllability mediates the relationship between rigid structure** 3 **and flexible dynamics**

4 **Shi Gu^{1,2,†}, Panagiotis Fotiadis^{2,3,†}, Linden Parkes², Cedric H. Xia⁴, Ruben C. Gur⁴, Raquel E. Gur⁴, David R.**
5 **Roalf⁴, Theodore D. Satterthwaite^{4,*}, and Danielle S. Bassett^{2,5-8,*}**

6 ¹Brain and Intelligence Group, School of Computer Science and Engineering, University of Electronic Science and Technology of China, Chengdu, China

7 ²Department of Bioengineering, University of Pennsylvania, Philadelphia, PA 19104, USA

8 ³Department of Neuroscience, Perelman School of Medicine, University of Pennsylvania, Philadelphia, PA 19104, USA

9 ⁴Department of Psychiatry, Perelman School of Medicine, University of Pennsylvania, Philadelphia, PA 19104, USA

10 ⁵Department of Electrical & Systems Engineering, University of Pennsylvania, Philadelphia, PA 19104, USA

11 ⁶Department of Physics & Astronomy, University of Pennsylvania, Philadelphia, PA 19104, USA

12 ⁷Department of Neurology, Perelman School of Medicine, University of Pennsylvania, Philadelphia, PA 19104, USA

13 ⁸Santa Fe Institute, Santa Fe, NM 87501, USA

14 ^{†,‡}Contributed equally to this work

15 ^{*}Corresponding Author

16 **Keywords:** Flexible Dynamics, Diffusion Tractography, Network Controllability, Network Modularity, Development

17 **ABSTRACT**

18 Precisely how the anatomical structure of the brain supports a wide range of complex functions remains a
19 question of marked importance in both basic and clinical neuroscience. Progress has been hampered by
20 the lack of theoretical frameworks explaining how a structural network of relatively rigid inter-areal
connections can produce a diverse repertoire of functional neural dynamics. Here, we address this gap by

21 positing that the brain's structural network architecture determines the set of accessible functional
22 connectivity patterns according to predictions of network control theory. In a large developmental cohort
23 of 823 youths aged 8 to 23 years, we found that the flexibility of a brain region's functional connectivity
24 was positively correlated with the proportion of its structural links extending to different cognitive
25 systems. Notably, this relationship was mediated by nodes' boundary controllability, suggesting that a
26 region's strategic location on the boundaries of modules may underpin the capacity to integrate
27 information across different cognitive processes. Broadly, our study provides a mechanistic framework
28 that illustrates how temporal flexibility observed in functional networks may be mediated by the
29 controllability of the underlying structural connectivity.

AUTHOR SUMMARY

30 Precisely how the relatively rigid white matter wiring of the human brain gives rise to a diverse repertoire
31 of functional neural dynamics is not well understood. In this work, we combined tools from network
32 science and control theory to address this question. Capitalizing on a large developmental cohort, we
33 demonstrated that the ability of a brain region to flexibly change its functional module allegiance over
34 time (i.e., its modular flexibility), was positively correlated with its proportion of anatomical edges
35 projecting to multiple cognitive networks (i.e., its structural participation coefficient). Moreover, this
36 relationship was strongly mediated by the region's boundary controllability, a metric capturing its
37 capacity to integrate information across multiple cognitive domains.

INTRODUCTION

38 The human brain is a complex interconnected system. Neural signals from one region spread to other
39 regions in the system by traveling through underlying nerve fibers. Conceptually, every function has its
40 foundation in structure (Huntenberg, Bazin, & Margulies, 2018; Park & Friston, 2013). Yet in practice, it
41 is methodologically challenging to construct interpretable and theoretically justified relations between
42 structure and function (Suarez, Markello, Betzel, & Misic, 2020). A key challenge lies in addressing
43 precisely how individual neural circuits interact with each other and thereby give rise to brain dynamics.

44 A second challenge lies in addressing the marked differences in structural and functional connectivity
45 fingerprints across individuals (Finn et al., 2015; S. Mueller et al., 2013).

46 A promising approach to meet these challenges is network neuroscience. Network neuroscience
47 utilizes graph theory to understand connectivity patterns in neural systems. The computational toolbox of
48 network neuroscience can be used to encode data acquired from multiple imaging modalities including
49 diffusion weighted imaging (DWI) and functional magnetic resonance imaging (fMRI) (Bassett &
50 Sporns, 2017). The former allows us to quantify the **structural connectivity** defined from axonal
51 projections, whereas the latter provides time series of the brain's blood-oxygen-level-dependent (BOLD)
52 activity that can be used to assess its **functional connectivity** (Bassett et al., 2011; Bullmore & Sporns,
53 2009; Hutchison et al., 2013). Therefore, network neuroscience equips us with a highly appropriate
54 framework to address our question on how the diverse functional expression of the human brain emerges
55 from its underlying structural architecture.

56 Although several prior studies have utilized graph theoretical principles to predict functional
57 connectivity given the underlying structural connectivity, it still remains unclear how relatively rigid
58 anatomical networks give rise to functional time series encoding flexible dynamic signals (Deco, Jirsa, &
59 McIntosh, 2011; Goñi et al., 2014; Hermundstad et al., 2013; Honey et al., 2009; Mišić et al., 2016; Park
60 & Friston, 2013; Supekar et al., 2010; Vasquez-Rodriguez et al., 2019). An early attempt to tackle this
61 problem focused on the statistical similarity between spatio-temporal structural and functional
62 connectivity patterns (Honey et al., 2009), and reported that functional patterns, although variable, are
63 constrained by the underlying structure. More recent studies have used principles from communication
64 theory to predict activity (Goñi et al., 2014), as well as to suggest that the transient nature of functional
65 connectivity depends on both the anatomical connections and the dynamic coordination of polysynaptic
66 pathways (Shen, Hutchison, Bezgin, Everling, & McIntosh, 2015). Complementary studies have also
67 begun to evaluate the relation between flexible functional expression and enhanced cognitive
68 performance (Baum et al., 2017, 2020; Bertolero, Yeo, & D'Esposito, 2015; Cocuzza, Ito, Schultz,
69 Bassett, & Cole, 2020; Cole, Ito, Cocuzza, & Sanchez-Romero, 2021; Hermundstad et al., 2013; Park &
70 Friston, 2013; Rosenberg, Martinez, et al., 2020; Rosenberg, Scheinost, et al., 2020; Sanchez-Alonso,
71 Rosenberg, & Aslin, 2021; Supekar et al., 2010; Wendelken et al., 2017; Yoo et al., 2020).

72 A crucial consideration when attempting to bridge structure and function is the identification of
73 descriptive statistics of network organization that can be translated from structural to functional
74 modalities (Cabral, Kringelbach, & Deco, 2017; Murphy, Bertolero, Papadopoulos, Lydon-Staley, &
75 Bassett, 2020). One such descriptive statistic considered in this work is **modular flexibility** (Khambhati,
76 Sizemore, Betzel, & Bassett, 2018). Modular flexibility represents how frequently brain regions change
77 the functional modules they belong to, across time. On a dynamic functional network, a region that is
78 more likely to be connected to multiple functional modules at different time-points is hence more
79 flexible. Indeed, modularity has been reported to flexibly vary across time in a manner that tracks
80 cognitive processes, including working-memory performance (Pedersen, Zalesky, Omidvarnia, &
81 Jackson, 2018), executive function (Baum et al., 2017), learning capability (Bassett et al., 2011),
82 attention (Shine, Koyejo, & Poldrack, 2016), ability to respond to environmental uncertainty (Kao et al.,
83 2020), and overall cognitive flexibility (Braun et al., 2015).

84 How does this flexible modularity arise from the relatively fixed white matter connectivity patterns? To
85 answer this question, we first turn to the way in which brain regions connect across modules. We use a
86 measure called the **participation coefficient**, which quantifies the relative distribution of a node's edges
87 between its own and different modules across the full brain network (Baum et al., 2017; Guimera &
88 Amaral, 2005; Power, Schlaggar, Lessov-Schlaggar, & Petersen, 2013). A lower participation coefficient
89 indicates that a node has edges primarily restricted to its own structural or functional **community**,
90 whereas a larger participation coefficient indicates that a node has edges uniformly distributed across
91 multiple communities (Power et al., 2013). To deepen our understanding, we next turn to a measure
92 called boundary controllability, recently introduced in the network control theory (NCT) literature
93 (Pasqualetti, Zampieri, & Bullo, 2014). The structural network architecture of a system, particularly as
94 measured by its **controllability**, can determine the range of dynamics that the system can support
95 (Towilson et al., 2018; Yan et al., 2017). Intuitively, structural boundary controllability measures the
96 necessary input required by a node to drive the overall system along a desired trajectory (Gu, Pasqualetti,
97 et al., 2015). The role of controllability in regulating dynamic brain state transitions as well as predicting
98 the maturity of adolescent brain systems during development has been corroborated by several recent
99 studies (Cornblath et al., 2020; Cui et al., 2020; Tang et al., 2017).

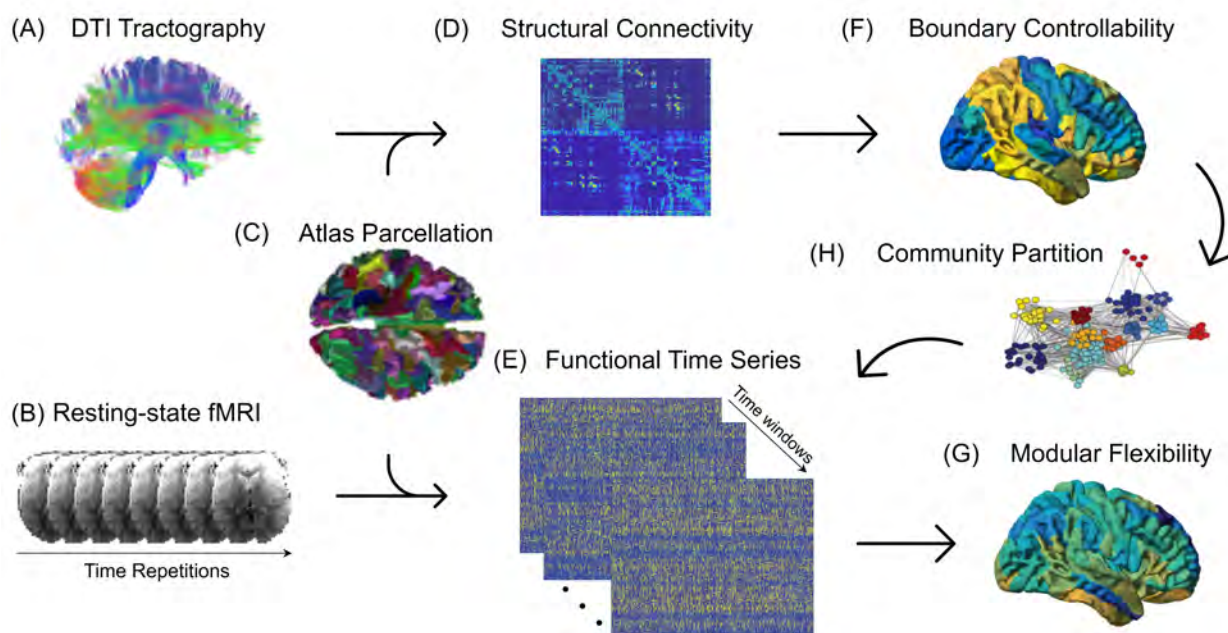
100 In the present work, we sought to understand the relationship between rigid structure and flexible
101 dynamics. Our approach was to examine the relationships between the participation coefficients of both
102 structural and functional networks, the boundary controllability of structural networks, and the modular
103 flexibility of dynamic functional networks, across regions and among individuals. We hypothesized that
104 the participation coefficients of the structural network architecture would positively correlate with the
105 corresponding flexibility of the functional network. Such a potential association is conceptually justified:
106 a node with edges connecting only to other nodes within its own module would not typically be expected
107 to suddenly alter its connectivity patterns and establish connections with nodes from different modules,
108 over a short period of time. Moreover, we theorized that this relationship between structural participation
109 coefficients and modular flexibility would be fully mediated by the serial effects of boundary
110 controllability and functional participation coefficients. By bridging structure to dynamics in this
111 step-wise fashion, we conceptually unpack the transfer function from rigidity to flexibility.

MATERIALS AND METHODS

112 *Data acquisition and pre-processing*

113 We used T1-weighted, diffusion tensor imaging (DTI) and resting-state fMRI BOLD data taken from 823
114 healthy individuals from the Philadelphia Neurodevelopmental Cohort (PNC) (Ingalhalikar et al., 2014;
115 Satterthwaite et al., 2014). All participants were between 8-23 years of age and their accompanying DTI
116 and fMRI data passed stringent quality control (Roalf et al., 2016; Rosen et al., 2018; Satterthwaite et al.,
117 2014, 2013). All MRI scans were acquired on the same 3T Siemens Tim Trio whole-body scanner with a
118 32-channel head coil at the Hospital of the University of Pennsylvania. The Institutional Review Boards
119 of both the University of Pennsylvania and the Children's Hospital of Philadelphia have approved the
120 study procedures.

127 The standardized structural imaging protocol included a T1-weighted scan obtained using a
128 magnetization-prepared, rapid-acquisition gradient-echo sequence (repetition time: TR = 1810ms, echo
129 time: TE = 3.5ms, field of view: FoV = 180 × 240mm², voxel dimensions = 1 × 1 × 1mm³, flip angle =
130 9°) and a DTI scan acquired using a twice-refocused spin-echo single-shot echo-planar imaging sequence
131 (TR = 8100ms, TE = 82ms, FoV = 240 × 240mm², voxel dimensions = 2 × 2 × 2mm³, flip angle =
132 90°/180°/180°). The T1-weighted scans were pre-processed using the automated *FreeSurfer* software



121 **Figure 1. Structural and Functional Processing Pipeline Schematic.** The (A) diffusive fiber tractography obtained from the DTI scans and (B) the resting-
 122 state BOLD fMRI time series are parcellated using (C) the 234-region Lausanne atlas, to construct (D) structural connectivity matrices and (E) functional
 123 time series for each subject. The structural connectivity matrices are then used to compute each region's (F) boundary controllability, whereas the functional
 124 time series are used to assess the modular dynamics of the time-resolved functional networks by calculating (G) the modular flexibility of each region. In our
 125 proposed analysis, the participation coefficients obtained from (H) the community partition of the static networks act as mediators in predicting how flexible
 126 the functional network will be, given its structural connections, thereby bridging the two imaging modalities.

133 suite (version 5.3) (Dale, Fischl, & Sereno, 1999; Fischl, Sereno, & Dale, 1999) and parcellated into 234
 134 individualized network nodes based on the Lausanne atlas (Cammoun et al., 2012). Each node was then
 135 assigned to one of eight pre-defined functional modules (Yeo et al., 2011): visual, somatomotor, dorsal
 136 attention, ventral attention, limbic, frontoparietal control, default mode network, and subcortical. The
 137 DTI scans were pre-processed using *FSL*, including skull stripping as well as correction for eddy currents
 138 and in-scanner motion (Smith et al., 2004). Deterministic tractography was then implemented using *DSI*
 139 *Studio*, and symmetric adjacency matrices were generated for each subject where the edge weight
 140 between two given nodes was defined as the mean **fractional anisotropy** along the connecting

141 streamlines (Yeh, Verstynen, Wang, Fernández-Miranda, & Tseng, 2014). A more detailed description of
142 the parameters used in the proposed processing pipeline can be found in Ref. (Baum et al., 2017).

143 Resting-state fMRI scans were also acquired for each subject using a BOLD sequence (TR = 3000ms,
144 TE = 32ms, FoV = 192 x 192mm², voxel dimensions = 3 x 3 x 3mm³, flip angle = 90°). The functional
145 images were pre-processed using a previously validated pipeline (Ciric et al., 2017). Steps included
146 correction for distortions induced by magnetic field inhomogeneities, removal of the initial four volumes
147 of each acquisition to allow for steady-state magnetization, re-alignment of all volumes to a reference
148 volume, co-registration of functional data to structural data, temporal band-pass filtering, and de-noising
149 (confound regression applied, including 36 regressors as well as spike regression) of the BOLD time
150 series (Ciric et al., 2017; Satterthwaite et al., 2013). In-scanner head motion was defined as the mean
151 relative root-mean-squared displacement calculated during the time series re-alignment step of the
152 pipeline (Satterthwaite et al., 2013). After the data were pre-processed, the scans were parcellated into
153 the same 234 individualized network nodes as the DTI scans. Functional connectivity matrices were
154 finally generated for each subject where the edge weight between two given nodes was defined as the
155 Pearson's correlation coefficient between their corresponding BOLD signals. The overall pipeline is
156 schematically illustrated in Figure 1.

157 *Participation Coefficients*

Participation coefficients measure the extent to which a node's connectivity profile participates diversely
across modules. Mathematically, given a network wherein N_m designates the total number of modules
considered (here set to eight), s iterates through the eight pre-defined functional modules mentioned in
the previous section, l_s^i represents the number of links between node i and nodes in module s , and
 $d_i = \sum_s l_s^i$ represents the total degree of node i , the participation coefficient of node i is defined as:

$$pc_i = 1 - \sum_{s=1}^{N_m} \left(\frac{l_s^i}{d_i} \right)^2. \quad (1)$$

158 Participation coefficients range between zero and one, where a value of zero indicates that a node's edges
159 are entirely restricted to its own community and a value of one indicates that a node's edges uniformly
160 extend across all other modules in the network (Power et al., 2013).

161 *Boundary Controllability of Structural Networks*

162 NCT is a mathematical framework that aims to assess whether a network can be controlled. Specifically,
163 NCT asks whether the output of the overall system can be driven towards a desired outcome given a set
164 of input signals. There are several metrics from NCT that attempt to quantify a node's overall ability to
165 alter other nodes' neurophysiological states (Pasqualetti et al., 2014). Here, we focused on a metric called
166 boundary controllability. Assuming we have a structural connectivity matrix constructed from a DTI
167 scan, the boundary controllability of a node is a heuristic metric predicting its ability to integrate
168 information across different cognitive processes. In other words, brain regions with high boundary
169 controllability tend to lie at the boundaries between network communities, and are thus thought to be
170 structurally predisposed to efficiently control the integration of different cognitive systems (Gu,
171 Pasqualetti, et al., 2015).

172 In order to calculate the boundary controllability of each brain region, we first partitioned the cortical
173 mantle into communities, using a common community-detection algorithm (Louvain-like locally greedy
174 heuristic algorithm) (Bassett et al., 2013; Blondel, Guillaume, Lambiotte, & Lefebvre, 2008; Gu,
175 Pasqualetti, et al., 2015). Based on that community partition, we identified an initial set of boundary
176 nodes (N_1) and assigned them a boundary controllability value of one (Pasqualetti et al., 2014). Then, we
177 used an iterative process to further partition the network into communities to identify more boundary
178 nodes at increasingly finer levels of the modular hierarchy, until all nodes were assigned a boundary
179 controllability value. During each step of this iterative process, the boundary controllability value of each
180 node i was set to $(N - N_i)/N$, where N is the total number of cortical brain regions and N_i is the
181 number of nodes on the boundary between communities (Gu, Pasqualetti, et al., 2015).

182 ***Modular Flexibility of Functional Networks***

183 Brain regions have been shown to interact among themselves across multiple temporal scales, even at rest
184 (Betz et al., 2019; Meunier, Lambiotte, Fornito, Ersche, & Bullmore, 2009; M. E. Newman, 2006;
185 Rubinov & Sporns, 2010). This property gives rise to modular dynamics which can be assessed
186 quantitatively by modular flexibility (Bassett et al., 2011).

The parcellated time series of each subject $\mathbf{x}_{N \times T}$ ($N = 234$ regions, $T = 120$ TRs) were divided into 10 non-overlapping time-windows, and the temporal network $\{A_{ijt}\}_{t=1}^{10}$ was constructed by defining A_{ijt} as the Pearson's correlation coefficient between the BOLD time series of regions i and j within the t^{th}

sliding window Telesford et al. (2016). Each time-window corresponded to a layer in the multi-layer network, and the multi-layer signed modularity function was defined as (Mucha, Richardson, Macon, Porter, & Onnela, 2010):

$$Q_{\text{multi-layer}} = \sum_{t=1}^T \sum_{ij} [(A_{ijt}^+ - \gamma P_{ijt}^+) - (A_{ijt}^- - \gamma P_{ijt}^-)] \delta(g_i^t, g_j^t) + \sum_{t=1}^{T-1} \sum_i \omega \cdot \delta(g_i^t, g_i^{t+1}), \quad (2)$$

187 where $A_{ijt} = A_{ijt}^+ - A_{ijt}^-$ is decomposed into its positive and negative parts with P_{ijt}^+ and P_{ijt}^-
 188 representing the corresponding parts obtained from null models (Newman-Girvan) (M. E. J. Newman &
 189 Girvan, 2004). The label g_i^t denotes the community assignment of node i in the t^{th} layer, $\delta(x, y)$ is the
 190 Kronecker- δ function set equal to 1 if $x = y$ and to 0 otherwise, γ is a parameter that tunes the size of
 191 communities (here, equal to 1), and ω represents the coupling strength between neighboring layers (here,
 192 equal to 1). A recent study identified that the test-retest reliability in calculating dynamic network
 193 measures, such as modular flexibility, depended on parameter selection (i.e., γ and ω), among other
 194 factors (Yang et al., 2020). Even though that study identified the parameter value pair with the overall
 195 highest intra-correlation coefficient to be $(\gamma, \omega) = (1.05, 2.05)$, we implemented the more widely used
 196 pair $(\gamma, \omega) = (1, 1)$ (Bassett et al., 2011; Betzel, Satterthwaite, Gold, & Bassett, 2017; Braun et al., 2015;
 197 Pedersen et al., 2018; Telesford et al., 2016) because the corresponding modular flexibility values were
 198 virtually identical ($r = 0.963, p = 0$).

In order to explore the temporal evolution of each module in the multi-layer network, each node within each time-window was assigned into a community, indicating its module allegiance. For this purpose, a Louvain-like locally greedy heuristic algorithm (Braun et al., 2015) was used to maximize the modularity index $Q_{\text{multi-layer}}$. This process gave rise to a partition matrix $\mathbf{G}_{N \times T}$ ($N = 234$ regions, $T = 10$ time-windows) in which $G_{i,t}$ represented the community to which node i in layer t belonged. The nodal flexibility f_i of each region i was then defined as:

$$f_i = 1 - \frac{1}{T-1} \sum_{t=1}^{T-1} \delta(G_{i,t}, G_{i,t+1}), \quad (3)$$

199 and assesses how often brain region i shifts its community assignment between temporal layers. On the
200 subject level, the global flexibility of the entire network was defined as the mean of all regional f_i values:
201 $F = \frac{1}{N} \sum_{i=1}^N f_i$. An in-depth description of the method can be found in Ref. (Khambhati et al., 2018).

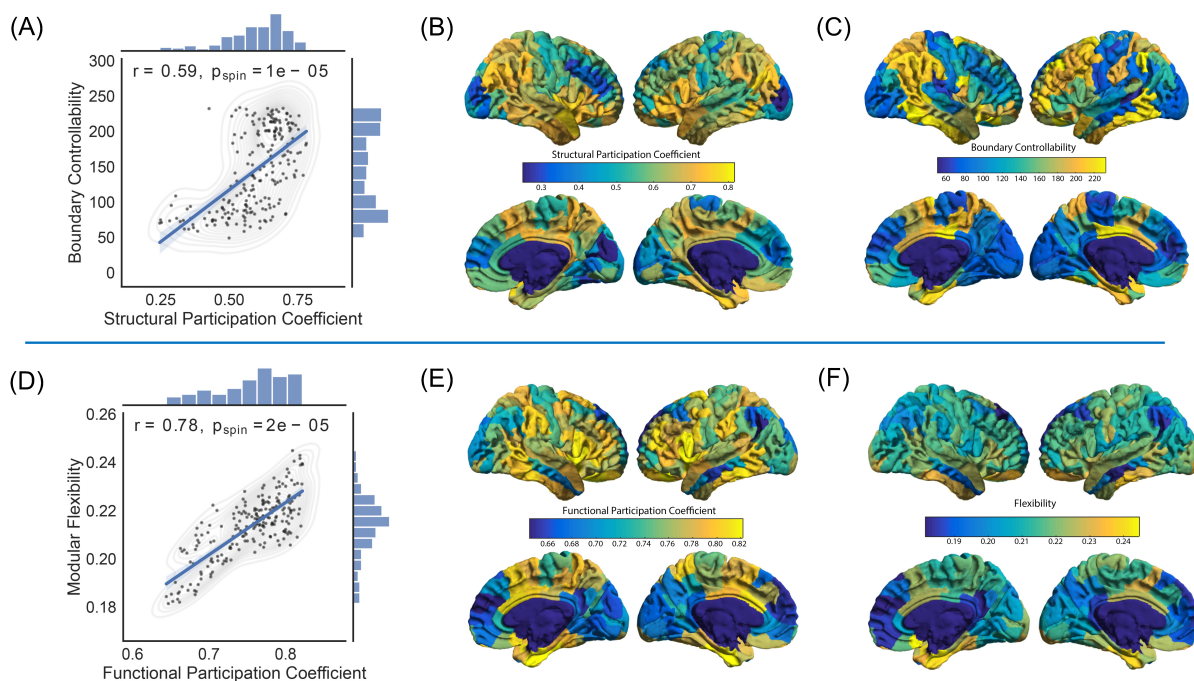
202 *Statistical Analyses*

203 All analyses were performed using the SPSS statistical software (v26, Armonk, NY: IBM Corporation)
204 and Python (v3.9). A threshold for significance of $p < 0.05$ was used. Pearson's correlation coefficients
205 (r) and p -values were reported for each bivariate analysis. In order to address the potential spatial
206 autocorrelation between our structural and functional metrics of interest, we applied a previously
207 validated spatial permutation framework (i.e., spin test with 100,000 permutations) to generate null
208 models (Alexander-Bloch et al., 2018). For those analyses (i.e., Figures 2A and D), the corresponding
209 p -values are reported as p_{spin} . Moreover, for all multiple linear regression analyses performed, age, sex,
210 and in-scanner head motion were adjusted for, and correction for multiple comparisons was performed
211 using the Benjamini-Hochberg false discovery rate (FDR) procedure (i.e., Figures 4 and 5) (Benjamini &
212 Hochberg, 1995).

213 *Mediation Model*

214 All mediation analyses were performed using the *PROCESS* (v3.4) statistical macro for SPSS (Hayes,
215 2017). Structural participation coefficients were designated as the independent variable, boundary
216 controllability as the first mediator, functional participation coefficients as the second mediator, and
217 modular flexibility as the dependent variable. Age, sex, and in-scanner head motion were used as
218 covariates in all subject-wide analyses. The hypothesized serial mediation effect was tested using
219 bootstrapping (10,000 samples). Mediation was deemed significant if the bootstrapping confidence
220 interval did not include zero. Unstandardized regression coefficients (c) and p -values were reported for
221 each association within the mediation analysis.

222 For the purpose of maintaining consistency, all variables within the mediation model were rescaled to
223 range from zero to one. Moreover, in order to incorporate temporal directionality into the model, the
224 functional participation coefficient of each node was calculated only during the first time-window of the



227 **Figure 2. Region-wide patterns.** Structural patterns are shown in the first row: (A) Boundary controllability was significantly correlated with the structural
228 participation coefficient ($r = 0.59$, $p_{spin} = 1 \times 10^{-5}$; the shaded areas correspond to the confidence curves for the fitted line). In order to address the
229 potential spatial autocorrelation between boundary controllability and the structural participation coefficient, we applied a spatial permutation framework (spin
230 test; see Methods). We also show the average patterns of regional fluctuations of (B) the structural participation coefficients and (C) boundary controllability,
231 across all subjects. Functional patterns are shown in the second row: (D) Modular flexibility was significantly correlated with the functional participation
232 coefficient ($r = 0.78$, $p_{spin} = 2 \times 10^{-5}$). In order to address the potential spatial autocorrelation between modular flexibility and the functional participation
233 coefficient, we applied a spatial permutation framework (spin test; see Methods). We also show the average patterns of regional fluctuations of (E) the functional
234 participation coefficients and (F) modular flexibility across all subjects.

225 resting-state fMRI BOLD sequence, whereas its modular flexibility was averaged across all remaining
226 time-windows (second through tenth).

RESULTS

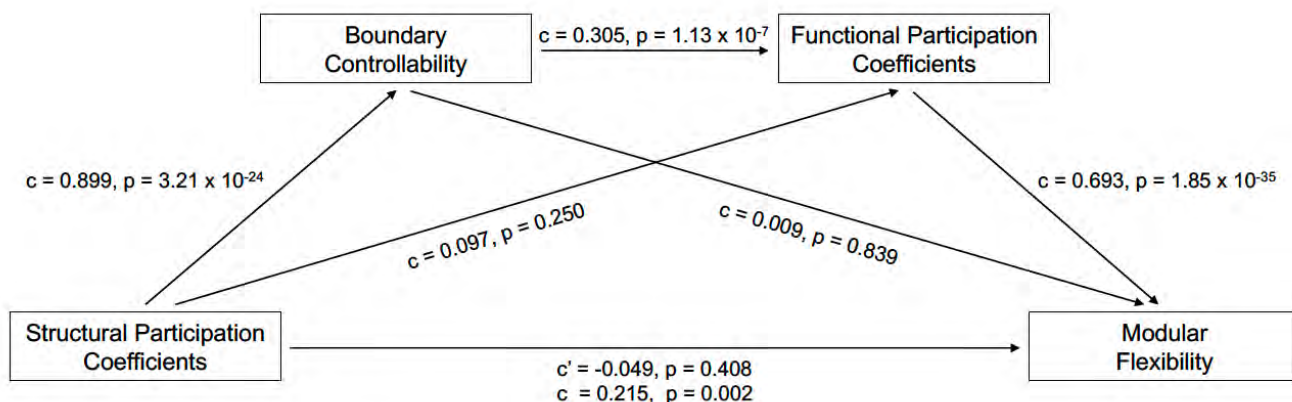
235 ***Structural Participation Coefficients Positively Correlate with Boundary Controllability***

236 A brain region's structural participation coefficient quantifies its role in communicating across multiple
237 modules (Hall et al., 2018). Similarly, boundary controllability assesses a region's predicted ability to
238 integrate information from different cognitive modules, attributing higher values to regions that are
239 located on the boundary of larger modules (Medaglia et al., 2018). Therefore, we hypothesized that these
240 two metrics would be positively correlated. To examine this hypothesis, we computed both metrics for
241 each region and averaged them across all subjects. We observed a strong positive correlation ($r = 0.59$,
242 $p_{spin} = 1 \times 10^{-5}$) between the structural participation coefficient and boundary controllability across
243 regions (Figure 2A). Regionally, the parietal and temporal lobes displayed high values of the
244 participation coefficient and boundary controllability, whereas the occipital lobe displayed low values
245 (Figures 2B and C).

246 ***Functional Participation Coefficients Positively Correlate with Modular Flexibility***

247 As described earlier, modular flexibility assesses how often a node shifts its community assignment
248 across different time-windows. Functional participation coefficients reflect the same property on the
249 static level; that is, during one time-window. Indeed, some regions known as connector hubs, play a
250 gating role across multiple communities and have a larger functional participation coefficient (Bertolero,
251 Yeo, Bassett, & D'Esposito, 2018; Cohen & D'Esposito, 2016). The same regions would also be
252 theoretically expected to often shift their allegiance between different cognitive networks, across multiple
253 temporal scales. Thus, we hypothesized that the participation coefficients obtained from the static
254 functional network would be positively correlated with the functional network's flexibility across time.
255 To test our hypothesis, we first computed these two metrics for each region and averaged the values
256 across subjects. We observed that the functional participation coefficients and the modular flexibility
257 were strongly positively correlated across regions ($r = 0.78$, $p_{spin} = 2 \times 10^{-5}$; Figure 2D). Moreover, the
258 temporal lobe displayed high values of functional participation coefficient and modular flexibility,
259 whereas the medial frontal lobe displayed low values (Figures 2E and F).

267 ***Boundary Controllability and Functional Participation Coefficients Serially Mediate the Relationship between***
268 ***Structural Participation Coefficients and Modular Flexibility***



260 **Figure 3. Serial Mediation Model.** We examined the hypothesis that the structural participation coefficient of each brain region (obtained from the DTI
 261 sequences) can predict its modular flexibility (obtained from the resting-state fMRI BOLD sequences) via the serial mediation effects of boundary controllability
 262 and the functional participation coefficient. In order to establish temporal directionality within the mediation model, the functional participation coefficient
 263 was calculated only during the first time-window of the functional time series and modular flexibility was averaged across all remaining time-windows (second
 264 through tenth). The unstandardized regression coefficient (c) and p -value are reported for each association within the mediation analysis. Moreover, the total
 265 and direct effects of the structural participation coefficient (independent variable) on modular flexibility (dependent variable) are also provided (total effect:
 266 regression coefficient c , p -value; direct effect: regression coefficient c' , p -value).

269 In the previous two sections, we established that a region's ability to dynamically interact with multiple
 270 cognitive modules (via structural controllability and functional flexibility) was also reflected on the static
 271 level (via participation coefficients), in both structural and functional modalities. We next attempted to
 272 bridge the two imaging modalities. We hypothesized that the structural participation coefficient of a
 273 region would predict its functional modular flexibility via the serial mediation effects of its boundary
 274 controllability and functional participation coefficient. In testing this hypothesis, we found that, across
 275 regions, the structural participation coefficient (the independent variable) was positively correlated with
 276 temporal modular flexibility (the dependent variable) ($r = 0.16, p_{spin} = 0.012$). As theorized, this effect
 277 was serially mediated by boundary controllability and functional participation coefficients (Figure 3; total
 278 effect = 0.215; $p = 0.002$, indirect effect = 0.190; Bootstrapping Confidence Interval = [0.119 0.269]).

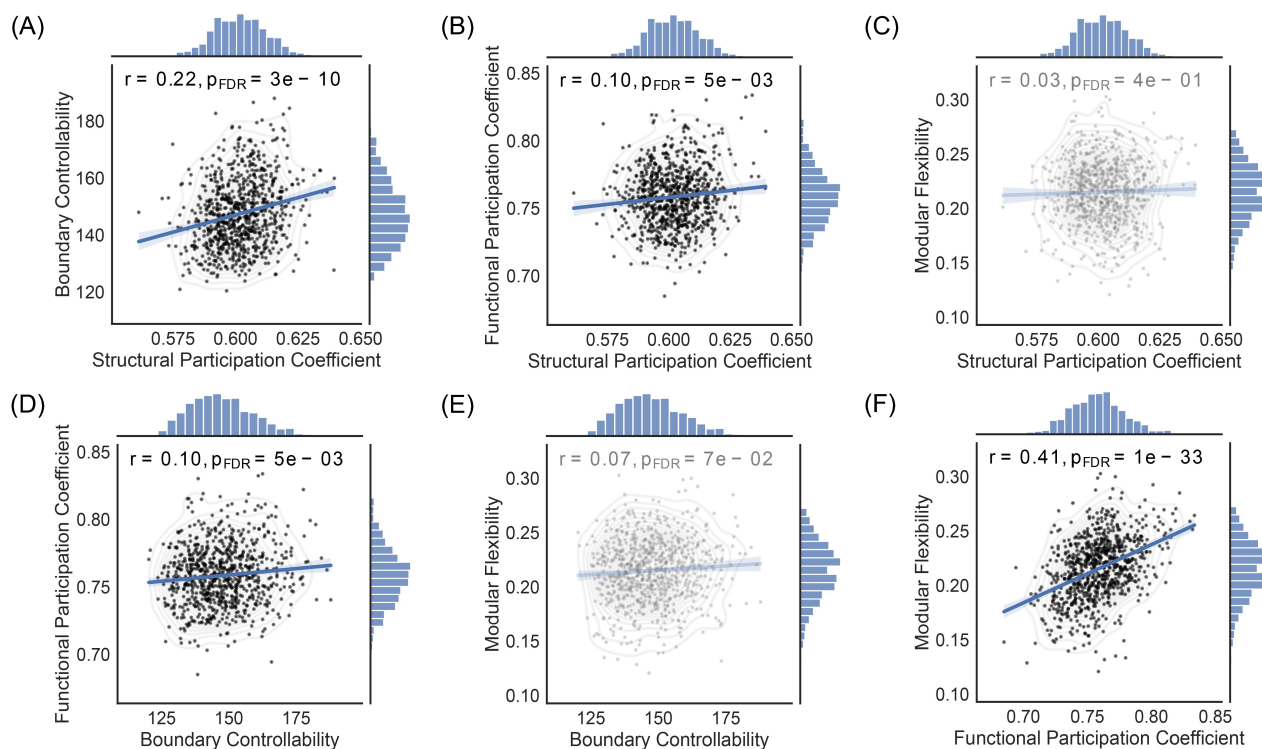
279 It is noteworthy that the significant positive correlation between structural participation coefficients
 280 and (the second mediator) functional participation coefficients ($r = 0.32, p = 3.88 \times 10^{-7}$) became

281 non-significant after regressing out (the first mediator) boundary controllability ($c = 0.097$; $p = 0.25$).
282 Similarly, even though the positive association between boundary controllability and modular flexibility
283 was significant ($r = 0.32$, $p = 5.54 \times 10^{-7}$), it became non-significant once the functional participation
284 coefficient was regressed out of the model ($c = 0.009$, $p = 0.84$). More importantly, however, the direct
285 effect of the structural participation coefficient on modular flexibility became non-significant once the
286 effects of the mediators were regressed out of the model (Figure 3; $c' = -0.049$, $p = 0.41$). These
287 statistical results strongly support the notion that the total effect of the structural participation coefficient
288 on modular flexibility is indeed fully mediated by the serial effects of boundary controllability and the
289 functional participation coefficient.

298 *Relationship between Participation Coefficients, Boundary Controllability, and Modular Flexibility, across*
299 *subjects*

300 Thus far, we have focused on regional variation in structure and dynamics, and their relations. Next, we
301 turn to subject-level variation to better understand inter-individual differences. Specifically, we examine
302 the relationship(s) between participation coefficients, boundary controllability, and modular flexibility,
303 across subjects. We used multiple linear regression models to adjust for age, sex, and in-scanner head
304 motion (corrected for multiple comparisons using FDR). As in the regional analyses, we observed that
305 the structural participation coefficient was positively correlated with boundary controllability (Figure 4A;
306 $r = 0.22$, $p = 3 \times 10^{-10}$; FDR) and with the functional participation coefficient (Figure 4B; $r = 0.10$,
307 $p = 0.005$; FDR), but not with modular flexibility (Figure 4C; $r = 0.03$, $p = 0.40$; FDR). Moreover,
308 boundary controllability was correlated with the functional participation coefficient (Figure 4D; $r = 0.10$,
309 $p = 0.005$; FDR) and had a trending association with modular flexibility (Figure 4E; $r = 0.07$, $p = 0.07$;
310 FDR). Lastly, we observed a strong positive correlation between average functional participation
311 coefficient and modular flexibility (Figure 4F; $r = 0.41$, $p = 1 \times 10^{-33}$; FDR). We note that in each
312 aforementioned multiple regression model, age was significantly and consistently correlated with the
313 dependent variable (Figure 4A: $p = 1.6 \times 10^{-7}$, Figure 4B: $p = 0.002$, Figure 4C: $p = 0.003$, Figure 4D:
314 $p = 0.002$, Figure 4E: $p = 0.007$, and Figure 4F: $p = 0.066$; FDR).

315 Although we observed no significant correlation between the structural participation coefficient and
316 modular flexibility across subjects, a mediation effect between the two variables could still exist (Hayes,



290 **Figure 4. Subject-wide correlations.** We examined whether the correlations observed within our structural and functional variables across regions persisted
291 across subjects. In all analyses, we adjusted for age, sex, and in-scanner head motion (FDR corrected for multiple comparisons). Here we show leverage
292 plots corresponding to the multiple linear regression models used: (A) The structural participation coefficient was significantly correlated with boundary
293 controllability ($r = 0.22$, $p = 3 \times 10^{-10}$) and with (B) the functional participation coefficient ($r = 0.10$, $p = 0.005$), but not with (C) modular flexibility
294 ($r = 0.03$, $p = 0.40$). (D) Global boundary controllability was also positively associated with the average functional participation coefficient for each subject
295 ($r = 0.10$, $p = 0.005$) and had a trending relationship with (E) modular flexibility ($r = 0.07$, $p = 0.07$). Lastly, as in the regional case, (F) each subject's
296 average functional participation coefficient was strongly correlated with its corresponding modular flexibility ($r = 0.41$, $p = 1 \times 10^{-33}$). The shaded areas
297 correspond to the confidence curves for the fitted lines.

317 2018). Thus, we examined whether boundary controllability and the functional participation coefficient
318 still played a serial mediation effect in regulating the relationship between the structural participation
319 coefficient and modular flexibility. Once again, we observed a significant mediation effect in the same
320 direction as observed in the regional analyses (total effect = 0.034, $p = 0.37$; indirect effect = 0.006;
321 Bootstrapping Confidence Interval = [0.0002 0.0125]). However, when age, sex, and in-scanner head

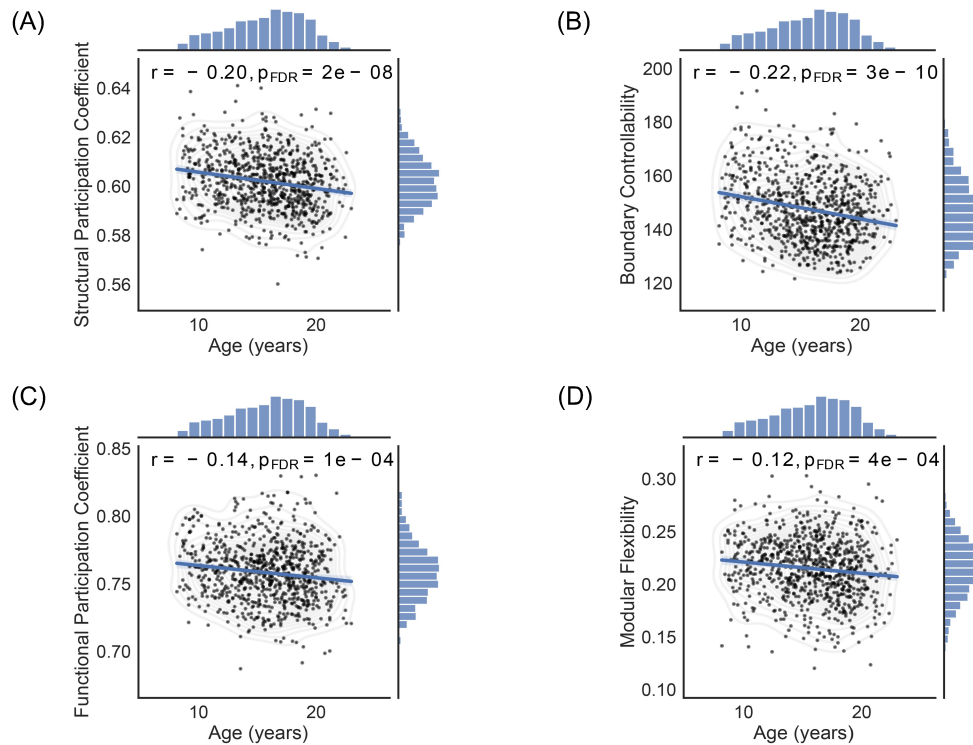
322 motion were also included as covariates in the mediation model, the significance disappeared (total effect
323 = -0.005, $p = 0.90$; indirect effect = 0.003; Bootstrapping Confidence Interval = [-0.001 0.009]).

324 *Developmental Trajectories of Participation Coefficients, Boundary Controllability, and Modular Flexibility*

325 Due to the substantial effects of age in the aforementioned subject-wide analyses, we tracked the
326 age-related changes in all pertinent variables. We specifically examined the relationships between age
327 and the structural and functional participation coefficients, boundary controllability, and modular
328 flexibility, after regressing out the effects of sex and in-scanner head motion (corrected for multiple
329 comparisons; FDR). Notably, all variables of interest decreased linearly with age, with the structural
330 markers (i.e., structural participation coefficient, Figure 5A, $r = -0.20$ and $p = 2 \times 10^{-8}$; boundary
331 controllability, Figure 5B, $r = -0.22$ and $p = 3 \times 10^{-10}$) displaying larger effect sizes than their
332 functional counterparts (i.e., functional participation coefficient, Figure 5C, $r = -0.14$ and
333 $p = 1 \times 10^{-4}$; modular flexibility, Figure 5D, $r = -0.12$ and $p = 4 \times 10^{-4}$).

DISCUSSION

339 The brain is an interconnected dynamical system whose functional expression relies on the underlying
340 white matter architecture (Deco et al., 2013). The intrinsic mechanisms, however, of how such a diverse
341 repertoire of functions emerges from a relatively rigid anatomical backbone have yet to be fully
342 understood. In this study, we combined tools from network neuroscience and control theory to examine
343 whether and how white matter tractography networks support the flexible modular architecture of the
344 brain, as derived from resting-state fMRI BOLD signals. In structural networks, we found that a region's
345 participation coefficient was strongly positively correlated with its boundary controllability, suggesting
346 that its ability to be controlled by external input can be assessed by the distribution of edges within its
347 own and different modules across the network. Similarly, in functional networks, we found that a region's
348 participation coefficient strongly correlated with its modular flexibility, suggesting that a region's
349 flexibility across multiple temporal windows can be captured by its static participation in the
350 communication occurring both within and between modules. Collectively, these observations provide us
351 with foundational intuitions regarding how temporally-evolving patterns of communication can arise
352 from fixed structural connectomes.



334 **Figure 5. Age-related changes in structural and functional metrics.** Global structural and functional metrics were derived per individual by averaging
335 the corresponding values across brain regions. (A) The structural participation coefficient ($r = -0.20$, $p = 2 \times 10^{-8}$; FDR), (B) boundary controllability
336 ($r = -0.22$, $p = 3 \times 10^{-10}$; FDR), (C) functional participation coefficient ($r = -0.14$, $p = 1 \times 10^{-4}$; FDR), and (D) modular flexibility ($r = -0.12$,
337 $p = 4 \times 10^{-4}$; FDR) all declined linearly with age. The effects of sex and in-scanner head motion were regressed out, and each analysis was FDR corrected
338 for multiple comparisons. The shaded areas correspond to the confidence curves for the fitted lines.

353 *Structure-function relations across anatomical regions*

354 Once a network structure is provided, one can begin to understand the anatomical support for various
355 patterns of communication both within and between its component modules (Avena-Koenigsberger,
356 Misisic, & Sporns, 2018). Each module (or community) consists of a group of densely interconnected
357 nodes (Sporns & Betzel, 2016). Each node can then be assigned a participation coefficient which
358 quantifies its connectivity distribution across communities (Guimera & Amaral, 2005). A high
359 participation coefficient indicates strong between-module and weak within-module connectivity; a low
360 participation coefficient indicates a more uniformly distributed connectivity pattern across modules.

361 Intuitively, whether a region's connections remain local to or expand beyond their community could
362 partially determine that region's control over signal transduction throughout the network (Gu, Pasqualetti,
363 et al., 2015; Medaglia et al., 2018). Here we validated that intuition in our structural analyses, where the
364 participation coefficient of a given node displayed a strong correlation with its boundary controllability.
365 The result also deepens our understanding of the brain's structural organization. The participation
366 coefficient is calculated from a single scale of modules as defined by the eight cognitive systems
367 examined (Yeo et al., 2011), whereas the boundary controllability assesses a region's location betwixt
368 modules defined across all scales, from eight modules to N modules. Hence, the strong relation between
369 these two variables indicates that submodules tend to be formed by larger modules breaking at a hinge,
370 rather than by the center of a large module falling out, like a donut hole. It would be interesting in future
371 work to further examine individual differences in these hinge-like hierarchies and assess their relevance
372 for cognitive function.

373 Whereas white matter structure provides anatomical support for communication patterns, the brain's
374 functional dynamics can provide more direct measurements of those putative patterns. In a functional
375 brain network, the participation coefficient can be used to assess how uniformly the edges of a node span
376 modules in a single temporal window, which is typically chosen to be the full duration of the functional
377 scan (Power et al., 2013). In contrast, modular flexibility can be used to assess how the allegiance of a
378 node to a module changes over multiple temporal windows, or over different time scales (Khambhati et
379 al., 2018). For instance, a node that constantly shifts its allegiance between different communities over a
380 task duration or resting-state period would have a high modular flexibility value. Flexibility is a
381 fundamental property of dynamical and adaptive systems, which is thought to support a range of human
382 cognitive processes including motivation (O'Ralley, 2020), working memory (Pedersen et al., 2018), and
383 cognitive flexibility (Braun et al., 2015; Ramos-Nunez et al., 2017), is age-dependent (Malagurski, Liem,
384 Oschwald, Merillat, & Janche, 2020; Schlesinger, Turner, Lopez, Miller, & Carlson, 2017), and can be
385 modulated by mood (Betzel et al., 2017), exercise (Sinha, Berg, Yassa, & Gluck, 2021), and hormonal
386 fluctuations (J. M. Mueller et al., 2021). Following existing literature discussing the relationship between
387 static and dynamic connectivity (Betzel, Fukushima, He, Zuo, & Sporns, 2016), we asked whether a
388 region's static participation coefficient was associated with its dynamic flexibility. That is, if a region is –
389 on average – strongly connected to multiple modules, does that region also have a propensity to change

390 the module to which it is most strongly connected over short time periods? We find that that answer is
391 “yes”: a region’s functional participation coefficient and modular flexibility were strongly positively
392 correlated. This correspondence between the temporal average and the time-resolved behavior provides
393 deeper insight into the nature of regional roles within a functional network. What appears over all
394 time-windows as a broad participation is in fact produced by temporally resolved affiliations, where a
395 region participates most closely with different modules at different time-points.

396 *What mediates the relationship between structure and dynamics?*

397 Given the cognitive and clinical relevance of flexibility (Bailey, Aboud, Nguyen, & Cutting, 2018;
398 Barbey, 2018; Bassett, Yang, Wymbs, & Grafton, 2015; Chong et al., 2019; Doucet, Bassett, Yao, Glahn,
399 & Frangou, 2017; Finc et al., 2017; Harlalka, Bapi, Vinod, & Roy, 2019; Rolls, Cheng, & Feng, 2021;
400 Shine, Bissett, et al., 2016; Zhang et al., 2016), it is important to establish a statistically principled
401 pathway whereby modular flexibility could be regulated, and might depend upon underlying structure.
402 Accordingly, we tested the hypothesis that a region’s structural participation coefficient predicts its
403 corresponding functional flexibility, via the serial mediation effects of its boundary controllability and
404 functional participation coefficient. In order to account for temporal directionality in this mediation
405 model, we computed each region’s functional participation coefficient only during the first time-window
406 (out of a total of 10 non-overlapping time-windows) of the resting-state fMRI BOLD sequence, and we
407 calculated its modular flexibility across all remaining time-windows of the same sequence. Consistent
408 with our hypothesis, we found a strong serial mediation effect between structural participation
409 coefficients and functional flexibility, which was fully mediated by the serial effects of boundary
410 controllability and functional participation coefficient (Figure 3). This directional mediation effect was
411 strong – yielding a ratio of indirect to total effect of 0.88 – in predicting the functional flexibility of a
412 region given its structural participation coefficient (Kenny, Kashy, & Bolger, 1998). Notably, when the
413 mediation effects of the two mediators were regressed out of the model, the significant association
414 between structural participation coefficients and modular flexibility disappeared, suggesting that a full
415 mediation effect was present (Hayes, 2018; Rucker, Preacher, Tormala, & Petty, 2011).

416 Overall, this result shows how a static structural property of a region can mediate a dynamic functional
417 property of the same region. Specifically, the distribution of a region’s edges at a given time-point can

418 mediate how a region shifts the edges' module allegiance over a period of time. Our observation that
419 boundary controllability and functional participation coefficients strongly mediated this relationship,
420 demonstrates that in addition to having edges reaching different modules across the network, a region's
421 strategic placement on the boundaries of such modules is also important in assessing its flexibility. This
422 dependence is intuitive, and existing on the boundary bestows the region with the ability to potentially
423 integrate information across different cognitive processes. Indeed, connector hubs – nodes with diverse
424 connections across modules and anatomically located at the boundaries between communities – have
425 been previously reported to coordinate connectivity changes occurring between nodes from different
426 communities, during cognitive tasks (Bertolero et al., 2018; Gratton, Laumann, Gordon, Adeyemo, &
427 Petersen, 2016).

428 *Structure-function relations across individuals & through development*

429 In order to examine how the relationships between participation coefficients, structural controllability,
430 and functional flexibility varied across participants, we computed a global average metric for each
431 structural and functional marker, per individual, and repeated the above analyses across a large
432 developmental cohort of youth (PNC) (Satterthwaite et al., 2014). Overall, the associations between the
433 variables of interest remained significant in multiple linear regression models adjusting for age, sex, and
434 in-scanner head motion, as in the region-wide analyses. There were, however, two main differences
435 between the across-region and the across-subjects results: (i) the relationship between the structural
436 participation coefficient and modular flexibility became non-significant in the across-subjects analysis,
437 and (ii) age was consistently correlated with the dependent variable in all regression models.

438 Even though there was no correlation between the structural participation coefficient and modular
439 flexibility in the across-subjects analysis, we re-tested our hypothesis that the relationship between the
440 two variables was still mediated by the structural networks' boundary controllability and the functional
441 networks' participation coefficients (Hayes, 2018). Similarly to the across-region analysis, we discovered
442 that a mediation effect of the same directionality was still present and significant. Notably, however,
443 when we included age as a covariate, the mediation effect was no longer significant. This observation
444 could reflect the instrumental role that age plays in shaping structural and functional connectivity during
445 this developmental period.

446 The important effect of age in the subject-wide mediation model, in addition to our earlier observation
447 that age was strongly correlated with each one of the variables explored in the subject-wide analyses,
448 motivated us to study the age-related changes in all structural and functional variables of interest. Such
449 changes are anticipated, given that the age range of our cohort spans childhood and adolescence, which is
450 a critical period of neurodevelopment and neuroplasticity (Brun et al., 2009; Casey, Tottenham, Liston, &
451 Durston, 2005; Foulkes & Blakemore, 2018; Fuhrmann, Knoll, & Blakemore, 2015; Lenroot et al., 2009;
452 Somerville et al., 2018). We found that both sets of structural (i.e., structural participation coefficient and
453 boundary controllability) and functional (i.e., functional participation coefficient and modular flexibility)
454 metrics decreased linearly with age, with the former displaying larger effect sizes.

455 The robust age-related decrease of the structural participation coefficient across youth observed in this
456 study has been previously reported (Baum et al., 2017; Dosenbach et al., 2010; Fair et al., 2009; Gu,
457 Satterthwaite, et al., 2015). As a region's participation coefficient decreases, it develops strong
458 within-module connectivity and weak between-module connectivity. The corresponding increase in
459 modular segregation across development has been shown to enhance network efficiency via the
460 strengthening of hub edges, and to support executive performance (Baum et al., 2017). Here we further
461 observe that boundary controllability decreases with age, while other metrics of controllability (average
462 and modal) have been reported to increase over the same developmental period (Tang et al., 2017). This
463 pattern of findings is particularly notable as boundary controllability is driven by changes in modular
464 architecture, whereas neurodevelopmental changes in average and modal controllability are not (Gu,
465 Pasqualetti, et al., 2015; Tang et al., 2017). These observations suggest that a fundamental change in
466 graph architecture is taking place throughout this developmental period that potentially contributes to the
467 maturity of brain modules, in support of the emergence of functional roles of cognitive systems (Gu,
468 Satterthwaite, et al., 2015) associated with network segregation (Baker et al., 2015; Baum et al., 2017;
469 Fair et al., 2009, 2007). Furthermore, the changes in modular flexibility that we observed across this
470 period could represent enhanced communication plasticity, paving the way for the emergence of
471 high-order cognitive functions characteristic of adulthood (Geerligs, Saliassi, Maurits, & Lorist, 2015;
472 Luna, Marek, Larsen, Tervo-Clemmens, & Chahal, 2015).

LIMITATIONS & FUTURE DIRECTIONS

473 The work should be examined in light of several methodological considerations and limitations. This
474 study, by design, was cross-sectional aiming to explore how functional flexibility emerged from the
475 underlying white matter architecture. A cross-sectional design is limited in its ability to tease apart
476 temporal precedence. As such, it would be highly informative to also include longitudinal data that
477 address how the structural and functional properties of each region change during this crucial period of
478 neurodevelopment. In order to account for temporal directionality in our mediation analyses, we
479 computed functional participation coefficients from the first temporal window of the fMRI BOLD
480 sequence and modular flexibility from the remaining time-windows. This approach could, however, raise
481 the issue that incorporating functional signals from a single time-window with limited time series length
482 could inflate signal noise (Noble, Scheinost, & Constable, 2019). In order to address this potential
483 concern, we repeated our mediation analyses after computing mean functional participation coefficients
484 and modular flexibility from all time-windows; all conclusions remained the same. Moreover, although
485 most of the structural and functional markers examined here have been separately reported to regulate
486 cognitive functions such as executive function (Baum et al., 2017; Reineberg & Banich, 2016),
487 processing speed (Varangis, Habeck, Razlighi, & Stern, 2019), and working memory (Stevens, Tappan,
488 Garg, & Fair, 2012), it would be beneficial to incorporate clinical and neurocognitive dimensions into our
489 mediation models. Incorporating behavioral data will address the question of how the serial mediation
490 model as a whole could shape behavior and cognition, and how deficits in the inter-relations among its
491 components could potentially lead to neurological and psychiatric developmental disorders (Aerts, Fias,
492 Caeyenberghs, & Marinazzo, 2016; Griffa, Baumann, Thiran, & Hagmann, 2013; Millan et al., 2012;
493 Warren et al., 2014). Finally, replicating our results in different cohorts during the same period would be
494 of paramount importance to ensure reproducibility.

CONCLUSION

495 In this study, we used tools from network neuroscience and control theory to examine how the brain's
496 relatively rigid white matter architecture gives rise to a diverse repertoire of flexible neural dynamics,
497 during normative development. We demonstrated that a brain region's ability to display temporal
498 flexibility in its functional expression positively correlated with the relative proportion of its anatomical
499 edges reaching different cognitive modules across the brain. Indeed, this relationship was strongly

500 mediated by the region's boundary controllability, that is its capacity to integrate information across
501 multiple cognitive processes. Overall, this work addresses the central question of how the human brain's
502 anatomical pathways support changes in flexible neural dynamics across late childhood, adolescence, and
503 early adulthood, and provides a framework that could be used to study how neurological and psychiatric
504 disorders emerge during that critical period of high neuroplasticity. Such analyses can leverage data on
505 neurocognitive performance and clinical features available on this sample.

AUTHOR CONTRIBUTIONS

506 Shi Gu: Conceptualization; Data curation; Analyses; Methodology; Visualization; Writing – original
507 draft; Writing – review & editing. Panagiotis Fotiadis: Conceptualization; Data curation; Analyses;
508 Methodology; Visualization; Writing – original draft; Writing – review & editing. Linden Parkes:
509 Conceptualization; Visualization; Writing – review & editing. Cedric H. Xia: Conceptualization;
510 Visualization; Writing – review & editing. David R. Roalf: Conceptualization; Writing - review &
511 editing. Ruben C. Gur: Conceptualization; Writing - review & editing. Raquel E. Gur:
512 Conceptualization; Writing - review & editing. Theodore D. Satterthwaite: Conceptualization;
513 Supervision; Funding Acquisition; Writing - review & editing. Danielle S. Bassett: Conceptualization;
514 Supervision; Funding Acquisition; Writing - review & editing.

FUNDING INFORMATION AND CONFLICTS OF INTEREST

515 Linden Parkes acknowledges support from the Brain & Behavior Research Foundation (2020 NARSAD
516 Young Investigator Grant). Ruben C. Gur and Raquel E. Gur acknowledge support from the National
517 Institutes of Health (R01 MH119219) and the Lifespan Brain Institute of Penn Medicine and Children's
518 Hospital of Philadelphia. David R. Roalf acknowledges support from the National Institute of Mental
519 Health (R01 MH119185, R01 MH120174) and the National Institute of Aging (R56 AG066656).
520 Theodore D. Satterthwaite and Danielle S. Bassett together acknowledge support from the National
521 Institutes of Health (R01 MH113550 and RF1 MH116920). Theodore D. Satterthwaite also
522 acknowledges support through NIH R01 MH120482. The authors declare no conflicts of interest.

CITATION DIVERSITY STATEMENT

523 Recent work in several fields of science has identified a bias in citation practices such that papers from
524 women and other minority scholars are under-cited relative to the number of such papers in the field
525 (Caplar, Tacchella, & Birrer, 2017; Dion, Sumner, & Mitchell, 2018; Dworkin et al., 2020; Maliniak,
526 Powers, & Walter, 2013; Mitchell, Lange, & Brus, 2013). We obtained the predicted gender of the first
527 and last author of each reference by using databases that store the probability of a first name being carried
528 by a woman (Dworkin et al., 2020). By this measure (and excluding self-citations to the first and last
529 authors of our current paper), our references contain 12.15% woman(first)/woman(last), 9.35%
530 man/woman, 23.36% woman/man, and 55.14% man/man. This method is limited in that a) names,
531 pronouns, and social media profiles used to construct the databases may not, in every case, be indicative
532 of gender identity and b) it cannot account for intersex, non-binary, or transgender people. We look
533 forward to future work that could help us better understand how to support equitable practices in science.

534

535 REFERENCES

536

- 537 Aerts, H., Fias, W., Caeyenberghs, K., & Marinazzo, D. (2016). Brain networks under attack: robustness properties and the
538 impact of lesions. *Brain*, *139*(12), 3063–3083.
- 539 Alexander-Bloch, A., Shou, H., Liu, S., Satterthwaite, T. D., Glahn, D. C., Shinohara, R. T., . . . Raznahan, A. (2018). On
540 testing for spatial correspondence between maps of human brain structure and function. *Neuroimage*, *178*, 540-551.
- 541 Avena-Koenigsberger, A., Misic, B., & Sporns, O. (2018). Communication dynamics in complex brain networks. *Nature*
542 *Reviews Neuroscience*, *19*(1), 17.
- 543 Bailey, S. K., Aboud, K. S., Nguyen, T. Q., & Cutting, L. E. (2018). Applying a network framework to the neurobiology of
544 reading and dyslexia. *Journal of Developmental Disorders*, *10*(37).
- 545 Baker, S. T., Lubman, D. I., Yücel, M., Allen, N. B., Whittle, S., Fulcher, B. D., . . . Fornito, A. (2015). Developmental
546 changes in brain network hub connectivity in late adolescence. *Journal of Neuroscience*, *35*(24), 9078-9087.
- 547 Barbey, A. K. (2018). Network neuroscience theory of human intelligence. *Trends in cognitive sciences*, *22*(1), P8-P20.

- 548 Bassett, D. S., Porter, M. A., Wymbs, N. F., Grafton, S. T., Carlson, J. M., & Mucha, P. J. (2013). Robust detection of
549 dynamic community structure in networks. *Chaos*, 23(1), 013142.
- 550 Bassett, D. S., & Sporns, O. (2017). Network neuroscience. *Nature neuroscience*, 20(3), 353.
- 551 Bassett, D. S., Wymbs, N. F., Porter, M. A., Mucha, P. J., Carlson, J. M., & Grafton, S. T. (2011). Dynamic reconfiguration
552 of human brain networks during learning. *Proceedings of the National Academy of Sciences*.
- 553 Bassett, D. S., Yang, M., Wymbs, N. F., & Grafton, S. T. (2015). Learning-induced autonomy of sensorimotor systems.
554 *Nature neuroscience*, 18(5), 744.
- 555 Baum, G. L., Ciric, R., Roalf, D. R., Betzel, R. F., Moore, T. M., Shinohara, R. T., . . . Satterthwaite, T. D. (2017). Modular
556 segregation of structural brain networks supports the development of executive function in youth. *Current Biology*,
557 27(11), 1561-1572.
- 558 Baum, G. L., Cui, Z., Roalf, D. R., Ciric, R., Betzel, R. F., Larsen, B., . . . Satterthwaite, T. D. (2020). Development of
559 structure–function coupling in human brain networks during youth. *Proceedings of the National Academy of Sciences*,
560 117(1), 771-778.
- 561 Benjamini, Y., & Hochberg, Y. (1995). Controlling the false discovery rate: A practical and powerful approach to multiple
562 testing. *Journal of the Royal Statistical Society*, 57(1), 289-300.
- 563 Bertolero, M. A., Yeo, B. T., & D’Esposito, M. (2015). The modular and integrative functional architecture of the human
564 brain. *Proceedings of the National Academy of Sciences*, 112(49), E6798-E6807.
- 565 Bertolero, M. A., Yeo, B. T. T., Bassett, D. S., & D’Esposito, M. (2018). A mechanistic model of connector hubs,
566 modularity and cognition. *Nature Human Behavior*, 2(10), 765-777.
- 567 Betzel, R. F., Bertolero, M. A., Gordon, E. M., Gratton, C., Dosenbach, N. U. F., & Bassett, D. S. (2019). The community
568 structure of functional brain networks exhibits scale-specific patterns of inter- and intra-subject variability. *Neuroimage*,
569 202, 115990.
- 570 Betzel, R. F., Fukushima, M., He, Y., Zuo, X.-N., & Sporns, O. (2016). Dynamic fluctuations coincide with periods of high
571 and low modularity in resting-state functional brain networks. *NeuroImage*, 127, 287-297.

- 572 Betzel, R. F., Satterthwaite, T. D., Gold, J. I., & Bassett, D. S. (2017). Positive affect, surprise, and fatigue are correlates of
573 network flexibility. *Scientific Reports*, 7, 520.
- 574 Blondel, V. D., Guillaume, J.-L., Lambiotte, R., & Lefebvre, E. (2008). Fast unfolding of communities in large networks.
575 *Journal of Statistical Mechanics: Theory and Experiment*, P10008.
- 576 Braun, U., Schäfer, A., Walter, H., Erk, S., Romanczuk-Seiferth, N., Haddad, L., . . . Bassett, D. S. (2015). Dynamic
577 reconfiguration of frontal brain networks during executive cognition in humans. *Proceedings of the National Academy of
578 Sciences*, 112(37), 11678-11683.
- 579 Brun, C., Lepore, N., Pennec, X., Lee, A. D., Barysheva, M., Madsen, S. K., . . . Thompson, P. M. (2009). Mapping the
580 regional influence of genetics on brain structure variability - a tensor-based morphometry study. *Neuroimage*, 48(1),
581 37-49.
- 582 Bullmore, E., & Sporns, O. (2009). Complex brain networks: graph theoretical analysis of structural and functional
583 systems. *Nature Reviews Neuroscience*, 10(3), 186.
- 584 Cabral, J., Kringelbach, M. L., & Deco, G. (2017). Functional connectivity dynamically evolves on multiple time-scales
585 over a static structural connectome: Models and mechanisms. *Neuroimage*, 160, 84-96.
- 586 Cammoun, L., Gigandet, X., Meskaldji, D., Thiran, J. P., Sporns, O., Do, K. Q., . . . Hagmann, P. (2012). Mapping the
587 human connectome at multiple scales with diffusion spectrum mri. *Journal of neuroscience methods*, 203(2), 386-397.
- 588 Caplar, N., Tacchella, S., & Birrer, S. (2017). Quantitative evaluation of gender bias in astronomical publications from
589 citation counts. *Nature Astronomy*, 1(6), 0141.
- 590 Casey, B., Tottenham, N., Liston, C., & Durston, S. (2005). Imaging the developing brain: what have we learned about
591 cognitive development? *Trends in cognitive sciences*, 9(3), 104-110.
- 592 Chong, J. S. X., Ng, K. K., Tandi, J., Wang, C., Poh, J.-H., & Zhou, H. J. (2019). Longitudinal changes in the cerebral
593 cortex functional organization of healthy elderly. *Journal of Neuroscience*, 39(28), 5534-5550.
- 594 Ciric, R., Wolf, D. H., Power, J. D., Roalf, D. R., Baum, G. L., Ruparel, K., . . . Satterthwaite, T. D. (2017). Benchmarking
595 of participant-level confound regression strategies for the control of motion artifact in studies of functional connectivity.
596 *Neuroimage*, 154, 174-187.

- 597 Cocuzza, C., Ito, T., Schultz, D., Bassett, D. S., & Cole, M. D. (2020). Flexible coordinator and switcher hubs for adaptive
598 task control. *Journal of Neuroscience*, *40*(36), 6949-6968.
- 599 Cohen, J. R., & D'Esposito, M. (2016). The segregation and integration of distinct brain networks and their relationship to
600 cognition. *Journal of Neuroscience*, *36*(48), 12083-12094.
- 601 Cole, M. W., Ito, T., Cocuzza, C., & Sanchez-Romero, R. (2021). The functional relevance of task-state functional
602 connectivity. *Journal of Neuroscience*, *41*(12), 2684-2702.
- 603 Cornblath, E. J., Ashourvan, A., Kim, J. Z., Betzel, R. F., Ciric, R., Adebimpe, A., . . . Bassett, D. S. (2020). Temporal
604 sequences of brain activity at rest are constrained by white matter structure and modulated by cognitive demands.
605 *Commun Biol*, *3*(1), 261.
- 606 Cui, Z., Stiso, J., Baum, G. L., Kim, J. Z., Roalf, D. R., Betzel, R. F., . . . Satterthwaite, T. D. (2020). Optimization of energy
607 state transition trajectory supports the development of executive function during youth. *Elife*, *9*, e53060.
- 608 Dale, A. M., Fischl, B., & Sereno, M. I. (1999). Cortical surface-based analysis. i. segmentation and surface reconstruction.
609 *Neuroimage*, *9*, 179-194.
- 610 Deco, G., Jirsa, V. K., & McIntosh, A. R. (2011). Emerging concepts for the dynamical organization of resting-state activity
611 in the brain. *Nature Reviews Neuroscience*, *12*(1), 43.
- 612 Deco, G., Ponce-Alvarez, A., Mantini, D., Romani, G. L., Hagmann, P., & Corbetta, M. (2013). Resting-state functional
613 connectivity emerges from structurally and dynamically shaped slow linear fluctuations. *Journal of Neuroscience*, *33*(27),
614 11239-11252.
- 615 Dion, M. L., Sumner, J. L., & Mitchell, S. M. (2018). Gendered citation patterns across political science and social science
616 methodology fields. *Political Analysis*, *26*(3), 312-327.
- 617 Dosenbach, N. U. F., Nardos, B., Cohen, A. L., Fair, D. A., Power, J. D., Church, J. A., . . . Schlaggar, B. L. (2010).
618 Prediction of individual brain maturity using fmri. *Science*, *329*, 1358-61.
- 619 Doucet, G. E., Bassett, D. S., Yao, N., Glahn, D. C., & Frangou, S. (2017). The role of intrinsic brain functional connectivity
620 in vulnerability and resilience to bipolar disorder. *American Journal of Neuropsychiatry*, *174*(12), 1214-1222.

- 621 Dworkin, J. D., Linn, K. A., Teich, E. G., Zurn, P., Shinohara, R. T., & Bassett, D. S. (2020). The extent and drivers of
622 gender imbalance in neuroscience reference lists. *Nature neuroscience*, *23*, 918–926.
- 623 Fair, D. A., Cohen, A. L., Power, J. D., Dosenbach, N. U., Church, J. A., Miezin, F. M., . . . Petersen, S. E. (2009).
624 Functional brain networks develop from a “local to distributed” organization. *PLoS computational biology*, *5*(5),
625 e1000381.
- 626 Fair, D. A., Dosenbach, N. U., Church, J. A., Cohen, A. L., Brahmbhatt, S., Miezin, F. M., . . . Schlaggar, B. L. (2007).
627 Development of distinct control networks through segregation and integration. *Proceedings of the National Academy of*
628 *Sciences*, *104*(33), 13507-13512.
- 629 Finc, K., Bonna, K., Lewandowska, M., Wolak, T., Nikadon, J., Dreszer, J., . . . Kuhn, S. (2017). Transition of the functional
630 brain network related to increasing cognitive demands. *Human Brain Mapping*, *38*, 3659–3674.
- 631 Finn, E. S., Shen, X., Scheinost, D., Rosenberg, M. D., Huang, J., Chun, M. M., . . . Constable, T. R. (2015). Functional
632 connectome fingerprinting: identifying individuals using patterns of brain connectivity. *Nature neuroscience*, *18*(11),
633 1664-1671.
- 634 Fischl, B., Sereno, M. I., & Dale, A. M. (1999). Cortical surface-based analysis. i. segmentation and surface reconstruction.
635 *Neuroimage*, *9*, 195-207.
- 636 Foulkes, L., & Blakemore, S.-J. (2018). Studying individual differences in human adolescent brain development. *Nature*
637 *neuroscience*, *21*, 315–323.
- 638 Fuhrmann, D., Knoll, L. J., & Blakemore, S.-J. (2015). Adolescence as a sensitive period of brain development. *Trends in*
639 *cognitive sciences*, *19*(10), P558-566.
- 640 Geerligs, R. J., Linda and Renken, Saliassi, E., Maurits, N. M., & Lorist, M. M. (2015). A brain-wide study of age-related
641 changes in functional connectivity. *Cerebral Cortex*, *25*, 1987–1999.
- 642 Goñi, J., van den Heuvel, M. P., Avena-Koenigsberger, A., de Mendizabal, N. V., Betzel, R. F., Griffa, A., . . . Sporns, O.
643 (2014). Resting-brain functional connectivity predicted by analytic measures of network communication. *Proceedings of*
644 *the National Academy of Sciences*, *111*(2), 833-838.
- 645 Gratton, C., Laumann, T. O., Gordon, E. M., Adeyemo, B., & Petersen, S. M. (2016). Evidence for two independent factors
646 that modify brain networks to meet task goals. *Cell Reports*, *17*(5), 1276-1288.

- 647 Griffa, A., Baumann, P. S., Thiran, J.-P., & Hagmann, P. (2013). Structural connectomics in brain diseases. *Neuroimage*, *80*,
648 515-526.
- 649 Gu, S., Pasqualetti, F., Cieslak, M., Telesford, Q. K., Alfred, B. Y., Kahn, A. E., . . . Bassett, D. S. (2015). Controllability of
650 structural brain networks. *Nature communications*, *6*, 8414.
- 651 Gu, S., Satterthwaite, T. D., Medaglia, J. D., Yang, M., Gur, R. E., Gur, R. C., & Bassett, D. S. (2015). Emergence of
652 system roles in normative neurodevelopment. *Proceedings of the National Academy of Sciences*, *112*(44), 13681-13686.
- 653 Guimera, R., & Amaral, L. A. (2005). Functional cartography of complex metabolic networks. *Nature*, *433*(7028), 895-900.
- 654 Hall, J. M., Shine, J. M., Ehgoetz Martens, K. A., Gilat, M., Broadhouse, K. M., Szeto, J. Y. Y., . . . Lewis, S. J. G. (2018).
655 Alterations in white matter network topology contribute to freezing of gait in parkinson's disease. *Journal of neurology*,
656 *265*(6), 1353-1364.
- 657 Harlalka, V., Bapi, R. S., Vinod, P. K., & Roy, D. (2019). Atypical flexibility in dynamic functional connectivity quantifies
658 the severity in autism spectrum disorder. *Frontiers in Human Neuroscience*, *13*(6).
- 659 Hayes, A. F. (2017). *Introduction to mediation, moderation, and conditional process analysis: A regression-based approach*
660 (2nd ed.). The Guilford Press.
- 661 Hayes, A. F. (2018). *Introduction to mediation, moderation, and conditional process analysis: A regression-based*
662 *approach*. The Guilford Press.
- 663 Hermundstad, A. M., Bassett, D. S., Brown, K. S., Aminoff, E. M., Clewett, D., Freeman, S., . . . Carlson, J. M. (2013).
664 Structural foundations of resting-state and task-based functional connectivity in the human brain. *Proceedings of the*
665 *National Academy of Sciences*, 201219562.
- 666 Honey, C., Sporns, O., Cammoun, L., Gigandet, X., Thiran, J.-P., Meuli, R., & Hagmann, P. (2009). Predicting human
667 resting-state functional connectivity from structural connectivity. *Proceedings of the National Academy of Sciences*,
668 *106*(6), 2035-2040.
- 669 Huntenberg, J. M., Bazin, P.-L., & Margulies, D. S. (2018). Large-scale gradients in human cortical organization. *Trends in*
670 *cognitive sciences*, *22*(1), 21-31.

- 671 Hutchison, M. R., Womelsdorf, T., Allen, E. A., Bandettini, P. A., Calhoun, V. D., Corbetta, M., . . . Chang, C. (2013).
672 Dynamic functional connectivity: promise, issues, and interpretations. *Neuroimage*, *80*, 360-378.
- 673 Ingalhalikar, M., Smith, A., Parker, D., Satterthwaite, T. D., Elliott, M. A., Ruparel, K., . . . Verma, R. (2014). Sex
674 differences in the structural connectome of the human brain. *Proceedings of the National Academy of Sciences*, *111*(2),
675 823-828.
- 676 Kao, C.-H., Khambhati, A. N., Bassett, D. S., Nassar, M. R., McGuire, J. T., Gold, J. I., & Kable, J. W. (2020). Functional
677 brain network reconfiguration during learning in a dynamic environment. *Nature communications*, *11*, 1682.
- 678 Kenny, D. F., Kashy, D. A., & Bolger, N. (1998). Handbook of social psychology. In D. Gilbert, S. Fiske, & G. Lindzey
679 (Eds.), (4th ed., p. 233-265). New York: McGraw-Hill.
- 680 Khambhati, A. N., Sizemore, A. E., Betzel, R. F., & Bassett, D. S. (2018). Modeling and interpreting mesoscale network
681 dynamics. *Neuroimage*, *180*(Pt B), 337-349.
- 682 Lenroot, R. K., Schmitt, J. E., Ordaz, S. J., Wallace, G. L., Neale, M. C., Lerch, J. P., . . . Giedd, J. N. (2009). Differences in
683 genetic and environmental influences on the human cerebral cortex associated with development during childhood and
684 adolescence. *Human Brain Mapping*, *30*, 163-174.
- 685 Luna, B., Marek, S., Larsen, B., Tervo-Clemmens, B., & Chahal, R. (2015). An integrative model of the maturation of
686 cognitive control. *Annual review of neuroscience*, *38*, 151-170.
- 687 Malagurski, B., Liem, F., Oswald, J., Merillat, S., & Janche, L. (2020). Longitudinal functional brain network
688 reconfiguration in healthy aging. *Human Brain Mapping*, *41*, 4829-4845.
- 689 Maliniak, D., Powers, R., & Walter, B. F. (2013). The gender citation gap in international relations. *International*
690 *Organization*, *67*(4), 889-922.
- 691 Medaglia, J. D., Harvey, D. Y., White, N., Kelkar, A., Zimmerman, J., Bassett, D. S., & Hamilton, R. H. (2018). Network
692 controllability in the inferior frontal gyrus relates to controlled language variability and susceptibility to tms. *Journal of*
693 *Neuroscience*, *38*(28), 6399-6410.
- 694 Meunier, D., Lambiotte, R., Fornito, A., Ersche, K. D., & Bullmore, E. T. (2009). Hierarchical modularity in human brain
695 functional networks. *Frontiers in Neuroinformatics*, *3*, 37.

- 696 Millan, M. J., Agid, Y., Brune, M., Bullmore, E. T., Carter, C. S., Clayton, N. S., . . . Young, L. J. (2012). Cognitive
697 dysfunction in psychiatric disorders: characteristics, causes and the quest for improved therapy. *Nature Reviews Drug*
698 *Discovery, 11*, 141-168.
- 699 Mišić, B., Betzel, R. F., De Reus, M. A., Van Den Heuvel, M. P., Berman, M. G., McIntosh, A. R., & Sporns, O. (2016).
700 Network-level structure-function relationships in human neocortex. *Cerebral Cortex, 26*(7), 3285-3296.
- 701 Mitchell, S. M., Lange, S., & Brus, H. (2013). Gendered citation patterns in international relations journals. *International*
702 *Studies Perspectives, 14*(4), 485-492.
- 703 Mucha, P. J., Richardson, T., Macon, K., Porter, M. A., & Onnela, J.-P. (2010). Community structure in time-dependent,
704 multiscale, and multiplex networks. *Science, 328*(5980), 876-878.
- 705 Mueller, J. M., Pritschet, L., Santander, T., Taylor, C. M., Grafton, S. T., Jacobs, E. G., & Carlson, J. M. (2021). Dynamic
706 community detection reveals transient reorganization of functional brain networks across a female menstrual cycle.
707 *Network Neuroscience, 5*(1), 125-144.
- 708 Mueller, S., Wang, D., Fox, M. D., Yeo, B. T. T., Sepulcre, J., Sabuncu, M. R., . . . Liu, H. (2013). Individual variability in
709 functional connectivity architecture of the human brain. *Neuron, 77*(3), 586-595.
- 710 Murphy, A. C., Bertolero, M. A., Papadopoulos, L., Lydon-Staley, D. M., & Bassett, D. S. (2020). Multimodal network
711 dynamics underpinning working memory. *Nature communications, 11*, 3035.
- 712 Newman, M. E. (2006). Modularity and community structure in networks. *Proceedings of the national academy of sciences,*
713 *103*(23), 8577-8582.
- 714 Newman, M. E. J., & Girvan, M. (2004). Finding and evaluating community structure in networks. *Physical Review E, 69,*
715 *026113*.
- 716 Noble, S., Scheinost, D., & Constable, T. R. (2019). A decade of test-retest reliability of functional connectivity: A
717 systematic review and meta-analysis. *Neuroimage, 203*, 116157.
- 718 O’Ralley, R. C. (2020). Unraveling the mysteries of motivation. *Trends in cognitive sciences, 24*(6), 425-434.
- 719 Park, H.-J., & Friston, K. (2013). Structural and functional brain networks: from connections to cognition. *Science,*
720 *342*(6158), 1238411.

- 721 Pasqualetti, F., Zampieri, S., & Bullo, F. (2014). Controllability metrics, limitations and algorithms for complex networks.
722 *IEEE: 2014 American Control Conference*, 3287-3292. doi: 10.1109/ACC.2014.6858621
- 723 Pedersen, M., Zalesky, A., Omidvarnia, A., & Jackson, G. D. (2018). Multilayer network switching rate predicts brain
724 performance. *Proceedings of the National Academy of Sciences*, 115(52), 13376-13381.
- 725 Power, J. D., Schlaggar, B. L., Lessov-Schlaggar, C. N., & Petersen, S. E. (2013). Evidence for hubs in human functional
726 brain networks. *Neuron*, 79(4), 798-813.
- 727 Ramos-Nunez, A. I., Fischer-Baum, S., Martin, R. C., Yue, Q., Ye, F., & Deem, M. W. (2017). Static and dynamic measures
728 of human brain connectivity predict complementary aspects of human cognitive performance. *Frontiers in Human
729 Neuroscience*, 11, 420.
- 730 Reineberg, A. E., & Banich, M. T. (2016). Functional connectivity at rest is sensitive to individual differences in executive
731 function: A network analysis. *Human Brain Mapping*, 37(8), 2959–2975.
- 732 Roalf, D. R., Quarmley, M., Elliot, M. A., Satterthwaite, T. D., Vandekar, S. N., Ruparel, K., . . . Gur, R. E. (2016). The
733 impact of quality assurance assessment on diffusion tensor imaging outcomes in a large-scale population-based cohort.
734 *Neuroimage*, 125, 903-919.
- 735 Rolls, E. T., Cheng, W., & Feng, J. (2021). Brain dynamics: the temporal variability of connectivity, and differences in
736 schizophrenia and adhd. *Translational Psychiatry*, 11(1), 70.
- 737 Rosen, A. F. G., Roalf, D. R., Ruparel, K., Blake, J., Seelaus, K., Villa, L. P., . . . Satterthwaite, T. D. (2018). Quantitative
738 assessment of structural image quality. *Neuroimage*, 169, 407-418.
- 739 Rosenberg, M. D., Martinez, S. A., Rapuano, K. M., Conley, M. I., Cohen, A. O., Cornejo, M. D., . . . Casey, B. (2020).
740 Behavioral and neural signatures of working memory in childhood. *Journal of Neuroscience*, 40(26), 5090-5104.
- 741 Rosenberg, M. D., Scheinost, D., Greene, A. S., Avery, E. W., Kwon, Y. H., Finn, E. S., . . . Chun, M. M. (2020). Functional
742 connectivity predicts changes in attention observed across minutes, days, and months. *Proceedings of the National
743 Academy of Sciences*, 117(7), 3797-3807.
- 744 Rubinov, M., & Sporns, O. (2010). Complex network measures of brain connectivity: uses and interpretations. *Neuroimage*,
745 52(3), 1059-1069.

- 746 Rucker, D. D., Preacher, K. J., Tormala, Z. L., & Petty, R. E. (2011). Mediation analysis in social psychology: Current
747 practices and new recommendations. *Social and Personality Psychology Compass*, 5(6), 359-371.
- 748 Sanchez-Alonso, S., Rosenberg, M. D., & Aslin, R. N. (2021). Functional connectivity patterns predict naturalistic viewing
749 versus rest across development. *Neuroimage*, 229, 117630.
- 750 Satterthwaite, T. D., Elliott, M. A., Ruparel, K., Loughhead, J., Prabhakaran, K., Calkins, M. E., . . . Gur, R. E. (2014).
751 Neuroimaging of the philadelphia neurodevelopmental cohort. *Neuroimage*, 86, 544-553.
- 752 Satterthwaite, T. D., Wolf, D. H., Ruparel, K., Erus, G., Elliott, M. A., Eickhoff, S. B., . . . Gur, R. C. (2013). Heterogeneous
753 impact of motion on fundamental patterns of developmental changes in functional connectivity during youth.
754 *Neuroimage*, 83, 45-57.
- 755 Schlesinger, K. J., Turner, B. O., Lopez, B. A., Miller, M. B., & Carlson, J. M. (2017). Age-dependent changes in
756 task-based modular organization of the human brain. *Neuroimage*, 146, 741-762.
- 757 Shen, K., Hutchison, R. M., Bezigin, G., Everling, S., & McIntosh, A. R. (2015). Network structure shapes spontaneous
758 functional connectivity dynamics. *Journal of Neuroscience*, 35(14), 5579-5588.
- 759 Shine, J. M., Bissett, P. G., Bell, P. T., Koyejo, O., Balsters, J. H., Gorgolewski, K. J., . . . Poldrack, R. A. (2016). The
760 dynamics of functional brain networks: integrated network states during cognitive task performance. *Neuron*, 92(2),
761 544-554.
- 762 Shine, J. M., Koyejo, O., & Poldrack, R. A. (2016). Temporal metastates are associated with differential patterns of
763 time-resolved connectivity, network topology, and attention. *Proceedings of the National Academy of Sciences*, 113(35),
764 9888-9891.
- 765 Sinha, N., Berg, C. N., Yassa, M. A., & Gluck, M. A. (2021). Increased dynamic flexibility in the medial temporal lobe
766 network following an exercise intervention mediates generalization of prior learning. *Neurobiology of Learning and*
767 *Memory*, 177, 107340.
- 768 Smith, S. M., Jenkinson, M., Woolrich, M. W., Beckmann, C. F., Behrens, T. E., Johansen-Berg, H., . . . Matthews, P. M.
769 (2004). Advances in functional and structural mr image analysis and implementation as fsl. *Neuroimage*, 23, S208-S219.
- 770 Somerville, L. H., Bookheimer, S. Y., Buckner, R. L., Burgess, G. C., Curtiss, S. W., Dapretto, M., . . . Barch, D. M. (2018).
771 The lifespan human connectome project in development: A large-scale study of brain connectivity development in 5-21

- 772 year olds. *Neuroimage*, 183, 456-468.
- 773 Sporns, O., & Betzel, R. F. (2016). Modular brain networks. *Annual review of psychology*, 67, 613-640.
- 774 Stevens, A. A., Tappon, S. C., Garg, A., & Fair, D. A. (2012). Functional brain network modularity captures inter- and
775 intra-individual variation in working memory capacity. *PLoS ONE*, 7(1), e30468.
- 776 Suarez, L. E., Markello, R. D., Betzel, R. F., & Misisic, B. (2020). Linking structure and function in macroscale brain
777 networks. *Trends in cognitive sciences*.
- 778 Supekar, K., Uddin, L. Q., Prater, K., Amin, H., Greicius, M. D., & Menon, V. (2010). Development of functional and
779 structural connectivity within the default mode network in young children. *Neuroimage*, 52(1), 290-301.
- 780 Tang, E., Giusti, C., Baum, G. L., Gu, S., Pollock, E., Kahn, A. E., . . . Bassett, D. S. (2017). Developmental increases in
781 white matter network controllability support a growing diversity of brain dynamics. *Nature Communications*, 8(1), 1252.
- 782 Telesford, Q. K., Lynall, M.-E., Vettel, J., Miller, M. B., Grafton, S. T., & Bassett, D. S. (2016). Detection of functional
783 brain network reconfiguration during task-driven cognitive states. *Neuroimage*, 142, 198-210.
- 784 Towilson, E. K., Vertes, P. E., Yan, G., Chew, Y. L., Walker, D. S., Schafer, W. R., & Barabasi, A.-L. (2018). *Caenorhabditis*
785 *elegans* and the network control framework-faqs. *Philosophical Transactions of the Royal Society B: Biological Sciences*,
786 373(1758), 20170372.
- 787 Varangis, E., Habeck, C. G., Razlighi, Q. R., & Stern, Y. (2019). The effect of aging on resting state connectivity of
788 predefined networks in the brain. *Frontiers in Aging Neuroscience*, 11(234).
- 789 Vasquez-Rodriguez, B., Suarez, L. E., Markello, R. D., Shafiei, G., Paquola, C., Hagmann, P., . . . Misisic, B. (2019).
790 Gradients of structure–function tethering across neocortex. *Proceedings of the National Academy of Sciences*, 116(42),
791 21219-21227.
- 792 Warren, D. E., Power, J. D., Bruss, J., Denburg, N. L., Waldron, E. J., Sun, H., . . . Tranel, D. (2014). Network measures
793 predict neuropsychological outcome after brain injury. *Proceedings of the National Academy of Sciences*, 111(39),
794 14247-14252.
- 795 Wendelken, C., Ferrer, E., Ghetti, S., Bailey, S. K., Cutting, L., & Bunge, S. A. (2017). Frontoparietal structural
796 connectivity in childhood predicts development of functional connectivity and reasoning ability: A large-scale

- 797 longitudinal investigation. *Journal of Neuroscience*, 37(35), 8549-8558.
- 798 Yan, G., Vertes, P. E., Towlson, E. K., Chew, Y. L., Walker, D. S., Schafer, W. R., & Barabasi, A.-L. (2017). Network
799 control principles predict neuron function in the caenorhabditis elegans connectome. *Nature*, 550(7677), 519-523.
- 800 Yang, Z., Telesford, Q. K., Franco, A., Gu, S., Xu, T., Ai, L., . . . Milham, M. P. (2020). Reliability of dynamic network
801 reconfiguration: impact of code implementation, parameter selection, scan duration, and task condition. *bioRxiv*.
- 802 Yeh, F.-C., Verstynen, T. D., Wang, Y., Fernández-Miranda, J. C., & Tseng, W.-Y. I. (2014). Deterministic diffusion fiber
803 tracking improved by quantitative anisotropy. *PLoS ONE*, 8(11), e80713.
- 804 Yeo, T. B. T., Krienen, F. M., Sepulcre, J., Sabuncu, M. R., Lashkari, D., Hollinshead, M., . . . Buckner, R. L. (2011). The
805 organization of the human cerebral cortex estimated by intrinsic functional connectivity. *Journal of Neurophysiology*,
806 106, 1125-1165.
- 807 Yoo, K., Rosenberg, M. D., Kwon, Y. H., Scheinost, D., Constable, R. T., & Chun, M. M. (2020). A cognitive state
808 transformation model for task-general and task-specific subsystems of the brain connectome. *bioRxiv*.
- 809 Zhang, J., Cheng, W., Liu, Z., Lei, X., Yao, Y., Becker, B., . . . Feng, J. (2016). Neural, electrophysiological and anatomical
810 basis of brain-network variability and its characteristic changes in mental disorders. *Brain*, 139(8), 2307–2321.